

1 **R methylCIPHER: A Methylation Clock Investigational Package for Hypothesis-
2 Driven Evaluation & Research**

3

4 Kyra L. Thrush^{1,2}, Albert T. Higgins-Chen^{3,4}, Zuyun Liu⁵, Morgan E. Levine^{2*}

5 ¹ Program in Computational Biology and Bioinformatics, Yale University, New Haven, CT, USA

6 ² Altos Labs, San Diego Institute of Science, San Diego, CA, USA

7 ³ Department of Psychiatry, Yale University School of Medicine, New Haven, CT, USA

8 ⁴ VA Connecticut Healthcare System, West Haven, CT, USA

9 ⁵ Center for Clinical Big Data and Analytics of the Second Affiliated Hospital and Department of Big Data in Health Science School
10 of Public Health, Zhejiang University School of Medicine, The Key Laboratory of Intelligent Preventive Medicine of Zhejiang

11 Province, Hangzhou, Zhejiang, China

12 * Corresponding Author

13 **Abstract**

14 **Background:** Epigenetic clocks are promising tools for the study of aging in humans.
15 The clocks quantify biological aging above and beyond chronological age, demonstrate
16 systematic associations with risk factors that accelerate aging, and predict age-related
17 morbidity and mortality. There is interest in using them as surrogate endpoints in
18 intervention studies. However, the large number of clocks, decentralized publication
19 and explosive popularity in the last decade has made for poor accessibility and
20 standardization. This has hampered the abilities of new researchers to conduct truly
21 hypothesis driven research—whether by not knowing about the best available clocks for
22 a given question, or by systematically testing many or all as they become available.

23 **Results:** We report a centralized R package which can be installed and run locally on
24 the user's machine, and provides a standardized syntax for epigenetic clock calculation.
25 The package includes a set of helper functions to assist with navigating clock literature
26 and selecting clocks for analysis, as well as affording the user with the details of clock

27 calculation. We describe each clock's resilience to missing CpG information, combined
28 with functionality to assess the need for imputation in the user's own data. Furthermore,
29 we demonstrate that while CpGs may not be shared among clocks with similar outputs,
30 many clocks have highly correlated outputs.

31 Conclusions: Due to the previous decentralization of epigenetic clocks, gathering code
32 and performing systematic analysis, particularly in protected datasets, has required
33 significant information gathering effort. Here, we offer an R package with standardized
34 implementation and potential for future growth and clock incorporation to assist with
35 hypothesis driven investigation of aging as measured by epigenetic clocks. We show
36 the potential of this package to drive the user to think globally about signals captured by
37 epigenetic clocks, as well as to properly identify the potential and limitations of each
38 clock in their current research.

39 **Keywords**

40

41 **Background**

42 Epigenetic clocks are promising tools, often discussed as future surrogate
43 biomarkers for studies of aging and longevity. These clocks have been extensively
44 reviewed; for their phenotypic associations [1, 2]; to understand the mechanisms of
45 epigenetic aging [3, 4]; [5][6] Our current intent is to instead provide a practical
46 overview of the categories, training methods, and applications of existing epigenetic
47 clocks. As epigenetic clock research gathers further momentum in the study of aging, it
48 is increasingly clear that a centralized toolkit to introduce the epigenetic clocks is
49 essential. Such a toolkit must satisfy, in our estimation, a handful of requirements: It

50 must (1) organize thematically and systematically the existing epigenetic clocks to
51 minimize the risks of multiple testing and publication bias; (2) provide functionality to
52 allow the researcher to perform not only *pro forma* analyses, implicating epigenetic
53 clocks in a disease or dataset of interest, but push researchers to glean further
54 biological insight as to the associations found; (3) be complete in its access of
55 epigenetic clocks, while still giving editorial insight such as to make use of them
56 navigable; (4) be sufficiently flexible so as to allow future advances to be made equally
57 accessible.

58 Because of the relative ease of training epigenetic clocks and of DNA
59 methylation (DNAm) collection, as well as the numerous age-related CpGs in the
60 genome, there are currently numerous human epigenetic clocks available in the
61 literature (Figure 1). The earliest such clocks utilize 1-10 highly age-associated CpGs in
62 regression models, and these remain useful as low-cost assays [7–11]. However, the
63 advent of large scale, streamlined collection of DNA methylation data on Illumina
64 Beadchip methylation array technologies, as well as the adoption of elastic-net
65 penalized regression to the training method, led to a new generation of clocks that can
66 capture genome-wide aging signals. The first of these were trained to predict
67 chronological age with high accuracy, including the Hannum blood [12] and Horvath
68 multi-tissue [13] clocks, and have since expanded to include additional clocks [14–17].
69 For those studying development and gestation, significant effort has been spent to
70 create reliable gestational and pediatric age clocks [18–22]. Similar approaches led to
71 the generation of mitotic clocks, so-called for their presumed ability to track the rate of
72 mitotic divisions and project cancer risk [23–25]. The telomere length estimator

73 DNAmTL, which is highly correlated with cellular replication rate, can be included in this
74 category as well [26].

75 In addition to clocks that predict discretely measurable aspects of age and cell
76 turnover, efforts have been made to capture heterogeneity in aging as meaningful
77 biological signal. These [27][28], and DunedinPACE[29] are trained to predict
78 individuals; degree or rate of biological change with time, especially those changes that
79 contribute to age-related morbidity and mortality risk. It has also been found that DNAm
80 can be used to predict various traits, lifestyles or exposures that are not necessarily
81 related to aging [30].

82 Finally, there has been recent interest in “bespoke” clocks designed for particular
83 tissues, diseases, data types, or applications. For example, one ongoing challenge for
84 epigenetic clocks is that most human clocks were trained using primarily whole blood[2].
85 Multi-tissue clocks[13]s conserved across tissues and may ignore tissue-specific aging
86 changes [6]. Thus, tissue-specific, bespoke clocks have been developed, including for
87 skin-and-blood [16], brain cortex [31], skin [32], and the scAge framework for predicting
88 epigenetic age from single cell methylation [33] have been reported. Also, since clocks
89 are often trained in large aging cohorts, it is possible they may miss aging patterns that
90 occur in small subsets of the population, as in the context of rare diseases. Due to the
91 increasing abundance of non-blood tissue DNAm, new methods for collection [34],
92 additional approaches to clock-training [35, 36], and emerging age-related diseases, we
93 predict that the number of bespoke clocks will see a dramatic increase in the next few
94 years.

95 Yet the challenge remains: Which clock should be used? The variety of
96 epigenetic clocks can be useful for investigating many different aspects of aging. But
97 selecting the appropriate clock(s) for a study requires navigating a decentralized body of
98 nuanced literature. The choice of clock may be impacted by the phenotype that they
99 were trained to predict or the context they were trained for. However, the differences
100 between clocks can be subtle, amounting to differences in training data composition or
101 procedure, such as age ranges [22], or preselection of CpGs [23].

102 This clock selection problem creates concerns regarding the integrity and
103 interpretability of aging studies. In particular, there are two consequences we would
104 hope to avoid. The first is exclusive, repeated testing of the best cited and most
105 reported aging clocks—namely the Horvath multi-tissue, Hannum, Levine PhenoAge
106 and GrimAge DNA methylation clocks. [1]. This aligns well with the plethora of
107 publications reporting the associations of acceleration of the Horvath multi-issue,
108 PhenoAge, and GrimAge predictors with biological changes[37–39], and disease risk or
109 mortality[40–45]. While this produces some standardization in the field, these clocks are
110 not necessarily the optimal choice in all cases. If a researcher instead has all available
111 clocks at their disposal and then applies a hypothesis-driven selection of clocks, an
112 alternative, lesser-known clock may indeed be the optimal choice. The second
113 unintended consequence could be that individuals test many clocks as clocks are
114 published or the researcher becomes aware of them, and only significant results tend to
115 be noted and published.

116 The variety of clocks and their decentralized distribution also creates practical
117 obstacles for aging research. Researchers wishing to apply epigenetic clocks must first

118 mine the literature for their options, identify one (or multiple) clocks to test, locate and
119 download the data to do so, and ensure that the calculation is properly performed
120 across their samples. This process creates substantial logistical barriers for
121 researchers. Clocks that are published along with public code and data should be
122 applauded. Furthermore, a few existing platforms can calculate multiple clocks. These
123 include the online Horvath calculator (<http://dnamage.genetics.ucla.edu>) and EstimAge
124 (<https://estimage.iac.rm.cnr.it>). However, these require data to be uploaded to a third
125 party server, which is prohibited for protected datasets and limits researchers' access to
126 the underlying details of calculation. There also exists the methylclock Bioconductor
127 package, which is currently limited to chronological age clocks, gestational age clocks,
128 DNAmTL and PhenoAge. In summary, the sheer number and variety of clocks creates
129 two primary challenges that impede use by the broader scientific community: (1) the
130 selection of the most appropriate clock(s) for the scientific question or hypothesis at
131 hand; (2) access to the many clocks. We address this by providing a centralized
132 resource in which individuals can explore, investigate, and calculate any and all clock(s)
133 appropriate for a research question from a project's inception. This is a necessary
134 improvement for the field, as it allows for systematic study of epigenetic clocks, which in
135 turn advances future understanding of their underlying relationships and biological
136 significance.

137 There is currently no true standard format or resource for the researcher to
138 publish and distribute clocks. Here we present a consolidated resource that applies a
139 standardized format to the calculation of epigenetic clocks, establishes a repository for
140 the fitted values of existing clocks, and provides a few helper functions for the

141 exploration of appropriate clocks, their CpGs, and inter-clock correlations. Further, this
142 package can be installed and run on a local machine, eliminating the need for uploading
143 of potentially protected data, and affords near-immediate results to the researcher,
144 regardless of the number or identity of clocks they choose to select. To further facilitate
145 accessibility of the epigenetic clocks, we have also provided a thorough tutorial walking
146 through use of the package and questions to be addressed on the github page for this
147 package (github.com/MorganLevineLab/methylCIPHER).

148 **Implementation**

149 *This should include a description of the overall architecture of the software
150 implementation, along with details of any critical issues and how they were addressed.*

151 The current package is implemented using the R programming language and
152 distributed via installation from Github (github.com/MorganLevineLab/methylCIPHER).
153 This distribution allows us to provide a flexible, regularly updated, and community driven
154 package. Not only can we push regular updates to users as new clocks are added, but
155 the research community can rapidly suggest new clocks, helper functions, or
156 improvements to code. Users wishing to generate their own independent Github R
157 packages during the publication process of novel clocks can be imported by this
158 package, or be referred to in the online Github based wiki and tutorial. The functions of
159 this package are represented in the schema in Figure 2.

160 To calculate epigenetic clocks in methylCIPHER (functions of the form *calc[Clock-*
161 *Name]*), the user provides a labeled data matrix of pre-processed methylation Beta
162 values obtained via the Illumina HumanMethylation450 Beadchip or Infinium
163 MethylationEPIC kit from Illumina (San Diego, CA). These are commonly referred to as

164 450k and EPIC arrays respectively. Preprocessing and normalization of methylation
165 data is typically performed within R using the *minfi* [46], *wateRmelon* [47], or *SeSAmE*
166 [48] packages, however methylCIPHER functions regardless of normalization protocol.
167 For more details regarding the effects of choice of normalization, refer to Ori et al. [49].
168 The user must simply have an object of *matrix* or *data frame* class, with named columns
169 corresponding to the Illumina CpG names, and cells containing methylation beta ratios
170 between 0 and 1.

171 We recommend that the methylation data object have named rows corresponding to
172 unique sample identifiers. Most analyses will benefit from a corresponding “phenotype”
173 data frame with sample identifiers; sample metadata; demographics; health outcomes;
174 age; sex; and other traits of interest. While optional for individual clock calculations, this
175 typically assists the researcher with downstream analyses. Without this data frame,
176 clocks can be computed using only a single function at a time, with output to a vector
177 object. However, the “pheno” dataframe provides a central location to append multiple
178 clocks to if using the multi-clock wrapper functions *calcUserClocks* or *calcCoreClocks*.

179 Of note, for some analyses (for example, calculation of IEAA or EEAA [50])
180 estimates of blood cell composition are necessary. To obtain such estimates, individuals
181 may want to use the Houseman method [51] of cell-type deconvolution from the *minfi*
182 package. However, local methods for predicting cell composition of blood can be
183 effectively run only when preprocessing occurs from raw methylation files (i.e. IDAT). If
184 access is limited to preprocessed methylation beta values, as in some publicly available
185 datasets, the Horvath Online calculator can predict blood component proportions. We
186 hope to provide users with this convenient functionality in the future. However, we have

187 provided a formatting function *formatHorvathOnline* which allows the user to quickly
188 generate the input files for the Horvath Online calculator. This allows for both calculation
189 of blood composition estimates and GrimAge [28].

190 The current version of the *R/methylCIPHER* package has been tested on both
191 Windows and Mac computer systems, running R v3.6+. It can run on most modern
192 personal computers, requiring less than 16 GB of RAM (and in many cases less than 8
193 GB) for methylation datasets containing hundreds of samples at once. The functions run
194 efficiently and will provide near-immediate results within seconds or minutes.

195 **Results & Discussion**

196 The R package *methylCIPHER* provides both seasoned and casual users of
197 epigenetic clocks with the tools necessary for thorough, hypothesis-driven research
198 using existing epigenetic clocks. We provide a comprehensive listing of human
199 epigenetic clocks that use; (1) linear approaches; and (2) CpGs found in the commonly
200 utilized Illumina 450k and EPIC arrays. This broad set of clocks can be searched
201 through the function *getClockOptions()*, which allows users to explore their options. We
202 have also provided convenient referencing of the source papers for each of the clock
203 calculation functions, using *citeMyClocks*. This accepts a group or list of functions at
204 once, which in turn allows readers to quickly refer to the original clock papers and
205 understand the underlying principles of their training. This process of information
206 gathering is shown graphically in the top right region of Figure 2.

207 Due to the variable performance of experimental designs, and a multitude of
208 existing pipelines for quality control, users may find missing probes or DNAm values in
209 their data. This can be seen as missing probe columns in the final normalized beta

210 value matrix, columns of *NA* values, or sporadic *NA* values in sample/ probe pairs. If the
211 probes are missing entirely from the beta value matrix, this can impact the decision to
212 implement specific clocks. Therefore, *getClockProbes* provides the user with a table to
213 determine what portion of probes are available for the various clock options, so that a
214 clearly informed decision can be made. Alternatively, they may find columns of all *NA*
215 values, which can be removed using *removeNAcol*. Sporadic missing values for select
216 probe/sample pairs can either be mean imputed across the matrix samples (using
217 function *meanimpute*), or imputation can be done later within the clock calculation
218 functions if a mean vector is provided as a reference containing the necessary CpGs.
219 However, most clocks can be calculated without imputation by simply ignoring those
220 CpGs in the resultant weighted regression values for such samples. The effect of doing
221 so varies by clock.

222 In figure 3 we visualize the degree of information contained in individual CpGs.
223 The model contribution of each CpG was estimated by multiplying the absolute
224 regression value in each clock for each site by its standard deviation in the Framingham
225 Heart Study (FHS) offspring cohort [52], and plotted against the standard deviation
226 alone. These results are shown for the Hannum (Figure 3A), Horvath Multi-Tissue
227 (Figure 3B), and PhenoAge (Figure 3C) clocks (additional clocks in supplemental
228 materials, figures S1-S2). With the CpGs plotted in this manner, we can see that each
229 CpG in the Hannum clock tends to have higher weight, evident from the higher mean
230 contribution represented by the blue horizontal dashed line. Further, PhenoAge employs
231 CpGs with higher standard deviation than the other clocks, but due to lower weight in
232 the clock regression, these tend to have dampened model contributions. These plots

233 help to conceptualize the effect of using mean imputation on model CpGs, as utilizing
234 mean imputation removes signal in individual samples that may reflect meaningful inter-
235 individual differences.

236 To functionalize this effect, we simulated the effects of increasing amounts of
237 missing array methylation probes for a given sample. We performed 1000 iterations
238 each of randomly drawing 0.01, 5, 10, and 20% of CpGs within each clock. Then, we
239 found the distribution of *Clock Years* information contained within each potentially
240 missing sample. Because we are approximating information lost, the *Clock Years*
241 measurement is defined by the absolute value of the sampled CpGs' clock regression
242 coefficient, multiplied by the standard deviation of these CpGs. The result is an
243 approximation of the information in years of measurement lost for a sample or set of
244 samples for which that proportion of CpGs's methylation is unavailable. We note that
245 because *Clock Years* is defined as absolute values for each CpG, oppositely weighted
246 CpGs in a clock do not counteract each other. Thus, the information lost may reflect a
247 larger difference than the shift in actual clock value. As each clock selected is of varying
248 size, the percentage of missing CpGs varies in the absolute number lost. Here, we
249 demonstrate that *Clock Years* information lost appears strongly associated with clock
250 size: Bigger clocks show a larger amount of information lost, despite removal of the
251 same proportion of sites (Figure 3D-F). However, as is demonstrated in the disparate
252 axis scaling between clocks, there must be far more CpGs missing to exert a similar
253 effect on the larger clocks than Hannum.

254 The user can choose, based on what is most appropriate for their hypothesis and
255 data available, a set of CpG-based DNA methylation clocks to calculate. Then, either

256 using the manual functions of the form `calc[Clock-Name]`, or a user-specific character
257 vector list of clocks, input to `calcUserClocks`, the appropriate values can be generated.
258 These are ideally output by binding to an existing “phenotype” data frame supplied by
259 the user containing relevant sample metadata.

260 To calculate each clock, an RData object is accessed containing CpG identity
261 and weight information as supplied by the original authors. Each of these objects can be
262 accessed using `data("[Clock-Name] CpG(s)")`. A central repository where these data
263 objects are readily accessible has two advantages. First, it makes the details of clock
264 calculation transparent to the user. Second, it facilitates studies of clock CpG identities
265 and their biological underpinnings.

266 For example, methylCIPHER allowed us to quantify the overlapping CpG
267 identities of clocks within some of the categories identified in Figure 1. It is often
268 discussed within the field that CpGs—at least those on the Illumina array
269 technologies—change in a concerted, multi-collinear manner with age. This has
270 motivated some of our prior approaches to clustering clock CpGs to ascertain
271 underlying biological signals or changes [53, 54]. We find that the vast majority of CpGs
272 selected by clocks do tend to be unique to those clocks, though a small subset of
273 methylation sites are common across many clocks within categories (Figure 4A-B).

274 Other observations, such as the fact that EpiTOC2 is a subset of the original EpiTOC
275 sites, or that DNAmTL is entirely unique in its CpG selections, are immediately obvious
276 from this analysis (Figure 4B). However, despite sparse overlap in clock CpGs, it
277 remains that these clocks’ sex-adjusted age accelerations (i.e., residuals of regressing
278 clock values onto sample age and sex) are typically quite correlated (Figure 4C).

279 In fact, it was recently reported that numerous combinations of CpGs can be
280 used to train epigenetic clocks across the epigenome, a concept which arises primarily
281 from this noted redundancy [55]. To further investigate the CpG identities of the clocks
282 as distributed by the original authors in our data files, we repetitively retrained multiple
283 well known epigenetic clocks. We performed this analysis in both a chronological aging
284 clock (Hannum) and a tissue specific aging clock (Horvath Skin & Blood). We first
285 generated an experimental design matrix (Figure 5A), which consists of 19x200 sample
286 cells. Each cell is the result of one of 19 bootstrapped samples of the training data
287 individuals drawn with replacement (for up to 6 draws of the same individual), and 1 of
288 200 versions of 10,000 CpGs drawn without replacement from the available probes on
289 the 450K array. The concept of bootstrapped samples for model training was inspired
290 by the original Hannum training method [12]. We used the original Hannum training
291 dataset [12], and the publicly available training datasets (supplemental materials, table
292 1A) from the original Horvath Skin & Blood clock publication.

293 Given each experimental matrix cell, we retrain the epigenetic clocks in the
294 sampled data, by applying elastic net penalized regression on chronological age. Elastic
295 net regression was performed with 10-fold cross validation and a 0.5 ratio of LASSO
296 and Ridge regression. All models were subsequently evaluated in an independent test
297 dataset consisting of either whole blood methylation data [56] or skin and fibroblast
298 datasets (supplemental materials, table 1B).

299 This analysis enabled comparison across randomly selected subsets of
300 individuals and/or CpGs on retrained clocks. The correlations of predicted age and true
301 age measures were visualized as density plots organized by sample bootstrap, for both

302 Hannum (Figure 5B) and Horvath Skin & Blood (Figure 5C). Training sample
303 correlations were verified normal distributions with high degree of correlation, while
304 independent test sample correlations for these models retained relatively high
305 correlations. Medians of each density plot (small vertical bars) are compared to the
306 original clock's correlation to age in the test dataset (large vertical bar). As is
307 demonstrated in the case of Hannum, while some CpG subsets produce models that
308 have correlation as low as 0.89 with chronological age, this is still a relatively high
309 correlation. Thus, while access to some CpGs improves model performance, the
310 improvement is modest. Furthermore, even when lists of CpGs are partially overlapped,
311 the degree of overlap in selected CpGs is lower than expected (Figure 3D). Therefore,
312 while some CpGs may contain relatively important information for age prediction, there
313 may be significant redundancy in DNA methylation, allowing high model correlation and
314 performance even with low shared identity of CpGs. It is also important to note that the
315 original Hannum methylation age clock used CpG preselection [12] whereas here we
316 are performing unsupervised selection. This may account for the overall slightly reduced
317 performance. However, we find it more promising that the spread of resultant
318 correlations in test data is relatively small, retaining correlations above 0.8 for the vast
319 majority of models. This high redundancy amongst CpGs may largely explain why
320 different clocks trained to predict the same outcome can have such sparse overlap in
321 their composition.

322 Similar results are found for a tissue specific aging clock, Horvath Skin & Blood
323 (Figure 3C,E). Here, we see that despite training and testing with half the sample size of
324 the original clock, more than 50% of the models outperform the original clock's

325 prediction in the test dataset. It has been demonstrated that there are measurable
326 differences in age related DNA methylation changes between tissues [57, 58].
327 Consequently, there may exist particular sets of CpGs which are essential to the
328 function of for tissue specific aging clocks [49]. However, our results suggest that the
329 majority of the CpGs have significant redundancy even for use in a tissue specific age
330 predictor. Again, the selected CpGs do not have significant overlap between lists,
331 despite them having significant overlap within a list across sample bootstraps (Figure
332 5E). Therefore, there may be many CpGs to select from for age prediction in tissue-
333 specific contexts, though given the limitations of the current training method, they may
334 not be truly tissue-specific merely single-tissue trained.

335 Beyond enabling characterization and investigation of the existing epigenetic
336 clocks' mechanics, the current package enables efficient comparison of desired clocks
337 with important biological phenotypes, biomarker data, or other sample metadata (Figure
338 6). Due to the rapid calculation of DNAm-based clocks in new data with automatic
339 appending of results to existing phenotype/ sample metadata, researchers can quickly
340 search for associations between outcomes or biomarkers, and clock scores.

341 Typically, the user will want to residualize the clock scores rather than using raw
342 scores, to assess the effects of age acceleration. We have left this step up to the user,
343 as details of correction for batch, sex, race, or other features tend to be dataset, and
344 use specific. For instructions on how to approach calculating age residuals, please refer
345 to the included tutorial or wiki on our GitHub distribution repository.

346 We find that we can rapidly uncover interesting results, such as univariate
347 associations between the cluster of accelerated mitotic clocks and cardiovascular

348 outcomes in the Framingham heart study (FHS) data (Figure 6A). Alternatively, we find
349 that the acceleration of BMI and Alcohol clocks by McCartney et al. [30] well surpass
350 the univariate associations found by other clock accelerations to cancer types and
351 stages in a subset of TCGA data (Figure 6B).

352 In nearly all cases, we do not recommend that the user calculate all clocks
353 available to them, as this introduces significant multiple testing. We have previously
354 shown that clocks can be driven by similar information content [53], highlighting the
355 potential utility of clustered-clock approaches. Typically the researcher would be best
356 served by selecting a hypothesis-driven subset of clocks: This would look like a single
357 clock tested from within a cluster (e.g. one mitotic clock) or calculating and reporting all
358 clocks and their agreement. However, we aim to show the ease with which few or all
359 clocks can be assessed using the *methylCIPHER* package, as well as to provide
360 resources to guide those decisions according to the high degree of correlation between
361 clocks, particularly relative to those of the traits of interest.

362 **Conclusions**

363 The current software is an important compendium of clocks currently distributed
364 through a wide variety of means. This reduces impediments to users, both in gathering
365 the data for calculation, and ensuring reproducible and accurate calculation. Further,
366 prior decentralized reporting and distribution of epigenetic clocks has led to the potential
367 for researchers to inadvertently conduct significant multiple testing, potentially without
368 proper correction: This can even occur throughout the course of a project in which the
369 researcher becomes aware of, and iteratively tests, additional epigenetic clocks.

370 Through the provision of standardized clock calculation functions, and tools to
371 rapidly investigate options available to the user, we aim to improve uptake of epigenetic
372 clocks while enhancing the reproducibility of DNAm clock-based studies in the future.
373 Further, as the current package is installed locally to one's personal computer or
374 computing cluster, it is possible to rapidly calculate several epigenetic clocks, even in
375 protected data. We intend to expand the clocks contained in this package in the future:
376 (1) The addition of future human DNAm (regression) based clocks to the present
377 researcher's toolkit will be essential; (2) Availability of mammalian arrays [34] will spur
378 the use of similarly implemented epigenetic clocks for nonhuman vertebrates, and
379 should also be included here; (3) The online tutorial provided in the currently discussed
380 Github repository will be further expanded according to developing practice and user
381 suggestions for standard features of epigenetic clock-based disease and trait analysis.
382 Due to their different operating requirements and less standardized implementation,
383 other forthcoming methods of epigenetic clock calculation are unlikely to be housed
384 within this package, but we will direct users to their own sources using our wiki and
385 tutorial pages. These include, but are not limited to, deep learning-based clock
386 approaches [35, 59], the next generation of low-noise clocks referred to as PC Clocks
387 [36], and single cell epigenetic clocks approaches [33].

388

Availability and Requirements

390 Project name: methylCIPHER

391 Project home page: github.com/MorganLevineLab/methylCIPHER

392 Operating system(s): tested on Mac OS 11+, with and without M1 chip, Windows

393 Programming Language: R 3.6.1+

394 Other requirements:

395 License: TBD

396 Any restrictions to use by non-academics: TBD

397

398 **List of abbreviations**

399

400 **Declarations**

401 *Ethics approval and consent to participate*

402 Not applicable

403 *Consent for publication*

404 Not applicable

405 *Availability of data and materials*

406 All data necessary for clock calculation is provided through the distributed package.

407 Datasets used for figures 4 and 6 were provided by the Framingham Heart Study (FHS)

408 Offspring Study Cohort and The Cancer Genome Atlas (TCGA). The data used for

409 Figures 4C and 6A in the current publication are based on the use of study data

410 downloaded from the dbGaP web site, under phs000724. TCGA data (Figure 6B) can

411 be downloaded via the GDC Data Portal (<https://portal.gdc.cancer.gov>).

412 *Competing interests*

413 The authors declare no competing interests.

414 *Funding*

415

416

Authors' contributions

417 KLT was responsible for conception, packaging of code, and writing the present
418 manuscript. AHC, ZL, and MEL contributed code and suggestions for clocks to include
419 within the package, and reviewed the manuscript.

420

Acknowledgements

421 All figures were created in whole or in part using Lucidchart.

422

References

423 1. Oblak L, van der Zaag J, Higgins-Chen AT, Levine ME, Boks MP. A systematic review of
424 biological, social and environmental factors associated with epigenetic clock acceleration.
425 Ageing Research Reviews. 2021;69:101348.

426 2. Horvath S, Raj K. DNA methylation-based biomarkers and the epigenetic clock theory of
427 ageing. Nature Reviews Genetics. 2018;19:371–84.

428 3. Seale K, Horvath S, Teschendorff A, Eynon N, Voisin S. Making sense of the ageing
429 methylome. Nature Reviews Genetics. 2022;0123456789.

430 4. Kabacik S, Lowe D, Fransen L, Leonard M, Ang SL, Whiteman C, et al. The relationship
431 between epigenetic age and the hallmarks of ageing in human cells. Nature Aging. 2022.
432 <https://doi.org/10.1038/s43587-022-00220-0>.

433 5. Field AE, Robertson NA, Wang T, Havas A, Ideker T, Adams PD. DNA Methylation Clocks in
434 Aging: Categories, Causes, and Consequences. Mol Cell. 2018;71:882–95.

435 6. Bell CG, Lowe R, Adams PD, Baccarelli AA, Beck S, Bell JT, et al. DNA methylation aging clocks:
436 Challenges and recommendations. Genome Biology. 2019;20:1–24.

437 7. Bocklandt S, Lin W, Sehl ME, Sánchez FJ, Sinsheimer JS, Horvath S, et al. Epigenetic Predictor
438 of Age. PLOS ONE. 2011;6:e14821.

439 8. Vidal-Bralo L, Lopez-Golan Y, Gonzalez A. Simplified assay for epigenetic age estimation in
440 whole blood of adults. Frontiers in Genetics. 2016;7 JUL:1–7.

441 9. Weidner CI, Lin Q, Koch CM, Eisele L, Beier F, Ziegler P, et al. Aging of blood can be tracked by
442 DNA methylation changes at just three CpG sites. Genome Biology. 2014;15.

443 10. Garagnani P, Bacalini MG, Pirazzini C, Gori D, Giuliani C, Mari D, et al. Methylation of ELOVL2
444 gene as a new epigenetic marker of age. Aging Cell. 2012;11:1132–4.

445 11. Zbieć-Piekarska R, Spólnicka M, Kupiec T, Makowska Z, Spas A, Parys-Proszek A, et al.
446 Examination of DNA methylation status of the ELOVL2 marker may be useful for human age
447 prediction in forensic science. Forensic Science International: Genetics. 2015;14:161–7.

448 12. Hannum G, Guinney J, Zhao L, Zhang L, Hughes G, Sadda SV, et al. Genome-wide
449 Methylation Profiles Reveal Quantitative Views of Human Aging Rates. Molecular Cell.
450 2013;49:359–67.

451 13. Horvath S. DNA methylation age of human tissues and cell types. Genome Biology.
452 2013;14:3156.

453 14. Lin Q, Weidner CI, Costa IG, Marioni RE, Ferreira MRP, Deary IJ, et al. DNA methylation
454 levels at individual age-associated CpG sites can be indicative for life expectancy. Aging.
455 2016;8:394–401.

456 15. Zhang Y, Wilson R, Heiss J, Breitling LP, Saum KU, Schöttker B, et al. DNA methylation
457 signatures in peripheral blood strongly predict all-cause mortality. Nature Communications.
458 2017;8.

459 16. Horvath S, Oshima J, Martin GM, Lu AT, Quach A, Cohen H, et al. Epigenetic clock for skin
460 and blood cells applied to Hutchinson Gilford Progeria Syndrome and ex vivo studies. Aging.
461 2018;10:1758–75.

462 17. Zhang Q, Vallerga CL, Walker RM, Lin T, Henders AK, Montgomery GW, et al. Improved
463 precision of epigenetic clock estimates across tissues and its implication for biological ageing.
464 Genome Medicine. 2019;11:54.

465 18. Bohlin J, Håberg SE, Magnus P, Reese SE, Gjessing HK, Magnus MC, et al. Prediction of
466 gestational age based on genome-wide differentially methylated regions. *Genome Biology*.
467 2016;17:1–9.

468 19. Knight AK, Craig JM, Theda C, Bækvad-Hansen M, Bybjerg-Grauholt J, Hansen CS, et al. An
469 epigenetic clock for gestational age at birth based on blood methylation data. *Genome Biology*.
470 2016;17:1–11.

471 20. Mayne BT, Leemaqz SY, Smith AK, Breen J, Roberts CT, Bianco-Miotto T. Accelerated
472 placental aging in early onset preeclampsia pregnancies identified by DNA methylation.
473 *Epigenomics*. 2017;9:279–89.

474 21. Lee Y, Choufani S, Weksberg R, Wilson SL, Yuan V, Burt A, et al. Placental epigenetic clocks:
475 Estimating gestational age using placental DNA methylation levels. *Aging*. 2019;11:4238–53.

476 22. McEwen LM, O'Donnell KJ, McGill MG, Edgar RD, Jones MJ, MacIsaac JL, et al. The PedBE
477 clock accurately estimates DNA methylation age in pediatric buccal cells. *Proc Natl Acad Sci U S
478 A*. 2020;117:23329–35.

479 23. Yang Z, Wong A, Kuh D, Paul DS, Rakyan VK, Leslie RD, et al. Correlation of an epigenetic
480 mitotic clock with cancer risk. *Genome Biology*. 2016;17:1–18.

481 24. Youn A, Wang S. The MiAge Calculator: a DNA methylation-based mitotic age calculator of
482 human tissue types. *Epigenetics*. 2018;13:192–206.

483 25. Teschendorff AE. A comparison of epigenetic mitotic-like clocks for cancer risk prediction.
484 *Genome Medicine*. 2020;12:56.

485 26. Lu AT, Seeboth A, Tsai PC, Sun D, Quach A, Reiner AP, et al. DNA methylation-based
486 estimator of telomere length. *Aging*. 2019;11:5895–923.

487 27. Levine ME, Lu AT, Quach A, Chen BH, Assimes TL, Bandinelli S, et al. An epigenetic
488 biomarker of aging for lifespan and healthspan. *Aging*. 2018;10:573–91.

489 28. Lu AT, Quach A, Wilson JG, Reiner AP, Aviv A, Raj K, et al. DNA methylation GrimAge
490 strongly predicts lifespan and healthspan. *Aging*. 2019;11:303–27.

491 29. Belsky DW, Caspi A, Corcoran DL, Sugden K, Poulton R, Arseneault L, et al. DunedinPACE, a
492 DNA methylation biomarker of the pace of aging. *Elife*. 2022;11:e73420.

493 30. McCartney DL, Hillary RF, Stevenson AJ, Ritchie SJ, Walker RM, Zhang Q, et al. Epigenetic
494 prediction of complex traits and death. *Genome Biol*. 2018;19:136.

495 31. Shireby GL, Davies JP, Francis PT, Burrage J, Walker EM, Neilson GWA, et al. Recalibrating
496 the epigenetic clock: implications for assessing biological age in the human cortex. *Brain*.
497 2020;:1–13.

498 32. Boroni M, Zonari A, Reis de Oliveira C, Alkatib K, Ochoa Cruz EA, Brace LE, et al. Highly
499 accurate skin-specific methylome analysis algorithm as a platform to screen and validate
500 therapeutics for healthy aging. *Clinical Epigenetics*. 2020;12:105.

501 33. Trapp A, Kerepesi C, Gladyshev VN. Profiling Epigenetic Age in Single Cells. *Nature Aging*.
502 2021;1:1189–201.

503 34. Arneson A, Haghani A, Thompson MJ, Pellegrini M, Kwon S bin, Vu H, et al. A mammalian
504 methylation array for profiling methylation levels at conserved sequences. *Nature
505 Communications*. 2022;13:1–13.

506 35. Galkin F, Mamoshina P, Kochetov K, Sidorenko D, Zhavoronkov A. DeepMAge: A
507 Methylation Aging Clock Developed with Deep Learning. *Aging Dis*. 2021;12:1252–62.

508 36. Higgins-chen AT, Thrush KL, Wang Y, Kuo P-L, Wang M, Minteer CJ, et al. A computational
509 solution for bolstering reliability of epigenetic clocks: Implications for clinical trials and
510 longitudinal tracking. *bioRxiv*. 2021.
511 <https://doi.org/https://doi.org/10.1101/2021.04.16.440205>.

512 37. Levine ME, Lu AT, Chen BH, Hernandez DG, Singleton AB, Ferrucci L, et al. Menopause
513 accelerates biological aging. *Proc Natl Acad Sci U S A*. 2016;113:9327–32.

514 38. Breitling LP, Saum KU, Perna L, Schöttker B, Holleczek B, Brenner H. Frailty is associated with
515 the epigenetic clock but not with telomere length in a German cohort. *Clinical Epigenetics*.
516 2016;8:1–8.

517 39. Simpkin AJ, Cooper R, Howe LD, Relton CL, Davey Smith G, Teschendorff A, et al. Are
518 objective measures of physical capability related to accelerated epigenetic age? Findings from a
519 British birth cohort. *BMJ Open*. 2017;7.

520 40. Beynon RA, Ingle SM, Langdon R, May M, Ness A, Martin RM, et al. Epigenetic biomarkers of
521 ageing are predictive of mortality risk in a longitudinal clinical cohort of individuals diagnosed
522 with oropharyngeal cancer. *Clinical Epigenetics*. 2022;14:1–13.

523 41. McCrory C, Fiorito G, Hernandez B, Polidoro S, O'Halloran AM, Hever A, et al. GrimAge
524 Outperforms Other Epigenetic Clocks in the Prediction of Age-Related Clinical Phenotypes and
525 All-Cause Mortality. *Journals of Gerontology - Series A Biological Sciences and Medical Sciences*.
526 2021;76:741–9.

527 42. Han LKM, Aghajani M, Clark SL, Chan RF, Hattab MW, Shabalin AA, et al. Epigenetic aging in
528 major depressive disorder. *American Journal of Psychiatry*. 2018;175:774–82.

529 43. Horvath S, Levine AJ. HIV-1 infection accelerates age according to the epigenetic clock.
530 *Journal of Infectious Diseases*. 2015;212:1563–73.

531 44. Marioni RE, Shah S, McRae AF, Ritchie SJ, Muniz-Terrera G, Harris SE, et al. The epigenetic
532 clock is correlated with physical and cognitive fitness in the Lothian Birth Cohort 1936.
533 *International Journal of Epidemiology*. 2015;44:1388–96.

534 45. Perna L, Zhang Y, Mons U, Holleczek B, Saum KU, Brenner H. Epigenetic age acceleration
535 predicts cancer, cardiovascular, and all-cause mortality in a German case cohort. *Clinical
536 Epigenetics*. 2016;8:1–7.

537 46. Fortin JP, Triche TJ, Hansen KD. Preprocessing, normalization and integration of the Illumina
538 HumanMethylationEPIC array with minfi. *Bioinformatics*. 2017;33:558–60.

539 47. Pidsley R, Y Wong CC, Volta M, Lunnon K, Mill J, Schalkwyk LC. A data-driven approach to
540 preprocessing Illumina 450K methylation array data. *BMC Genomics*. 2013;14.

541 48. Zhou W, Triche Jr TJ, Laird PW, Shen H. SeSAMe: reducing artifactual detection of DNA
542 methylation by Infinium BeadChips in genomic deletions. *Nucleic Acids Research*.
543 2018;46:e123–e123.

544 49. Ori APS, Lu AT, Horvath S, Ophoff RA. A systematic evaluation of 41 DNA methylation
545 predictors across 101 data preprocessing and normalization strategies highlights considerable
546 variation in algorithm performance. *bioRxiv*. 2021;:2021.09.29.462387.

547 50. Horvath S, Ritz BR. Increased epigenetic age and granulocyte counts in the blood of
548 Parkinson's disease patients. *Aging*. 2015;7:1130–42.

549 51. Houseman EA, Accomando WP, Koestler DC, Christensen BC, Marsit CJ, Nelson HH, et al.
550 DNA methylation arrays as surrogate measures of cell mixture distribution. *BMC Bioinformatics*.
551 2012;13.

552 52. Kannel WB, Feinleib M, McNamara PM, Garrison RJ, Castelli WP. An Investigation of
553 Coronary Heart Disease in Families: The Framingham Offspring Study. *American Journal of*
554 *Epidemiology*. 1979;110:281–90.

555 53. Liu Z, Leung D, Thrush K, Zhao W, Ratliff S, Tanaka T, et al. Underlying features of epigenetic
556 aging clocks in vivo and in vitro. *Aging Cell*. 2020; March:1–11.

557 54. Levine M, Higgins-Chen AT, Thrush K, Minteer CJ, Niimi P. Clock Work: Deconstructing the
558 Epigenetic Clock Signals in Aging, Disease, and Reprogramming. *bioRxiv*.
559 2022;:2022.02.13.480245.

560 55. Porter HL, Brown CA, Roopnarinesingh X, Giles CB, Georgescu C, Freeman WM, et al. Many
561 chronological aging clocks can be found throughout the epigenome: Implications for
562 quantifying biological aging. *Aging Cell*. 2021;20:1–13.

563 56. Horvath S, Zhang Y, Langfelder P, Kahn RS, Boks MPM, van Eijk K, et al. Aging effects on DNA
564 methylation modules in human brain and blood tissue. *Genome Biol*. 2012;13:R97–R97.

565 57. Maegawa S, Hinkal G, Kim HS, Shen L, Zhang L, Zhang J, et al. Widespread and tissue specific
566 age-related DNA methylation changes in mice. *Genome Research*. 2010;20:332–40.

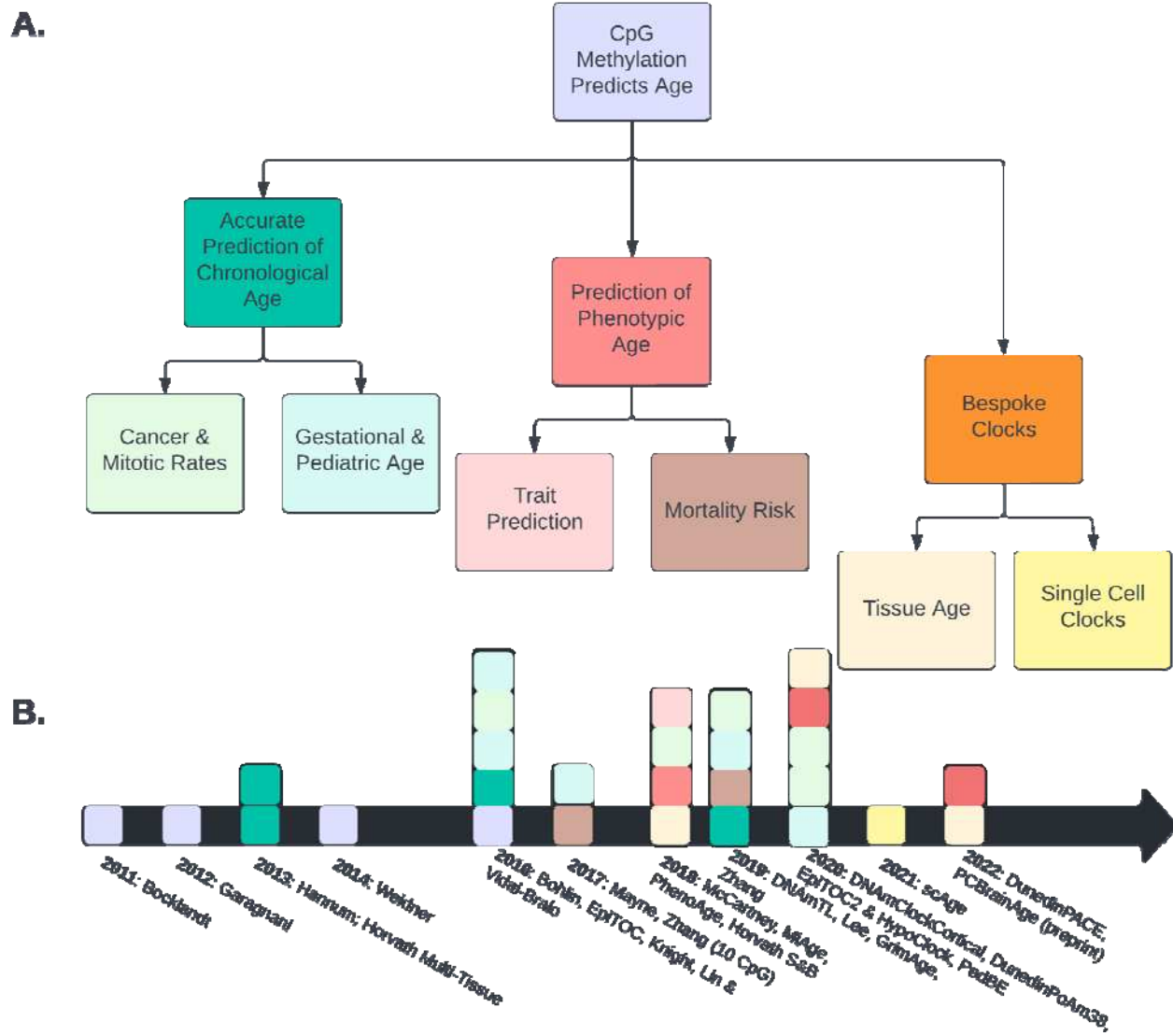
567 58. Day K, Waite LL, Thalacker-Mercer A, West A, Bamman MM, Brooks JD, et al. Differential
568 DNA methylation with age displays both common and dynamic features across human tissues
569 that are influenced by CpG landscape. *Genome Biology*. 2013;14:1.

570 59. de Lima Camillo LP, Lapierre LR, Singh R. AltumAge: A Pan-Tissue DNA-Methylation
571 Epigenetic Clock Based on Deep Learning. *bioRxiv*. 2021;:2021.06.01.446559.

572

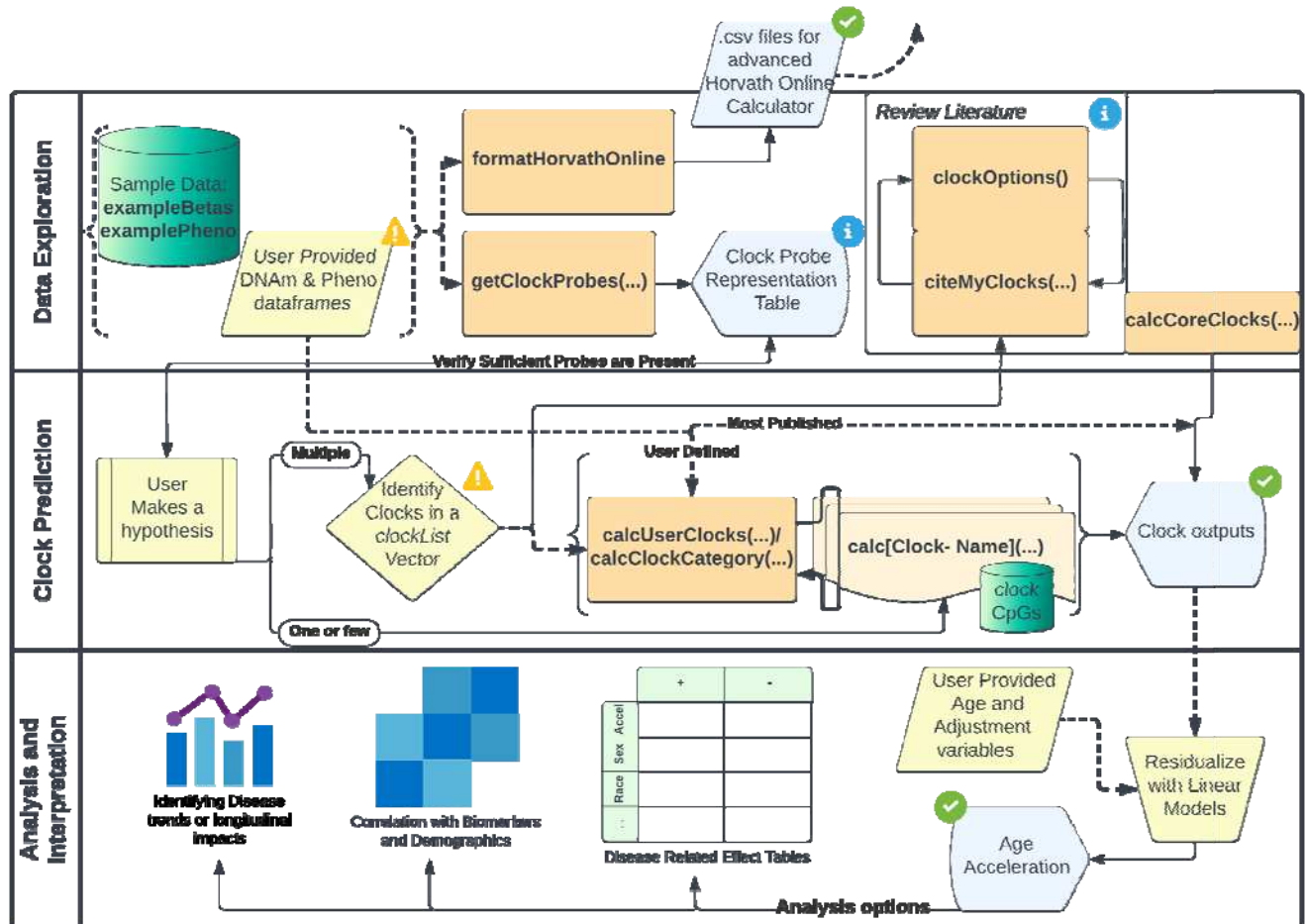
573 **Figures, Tables, and Additional Files**

574



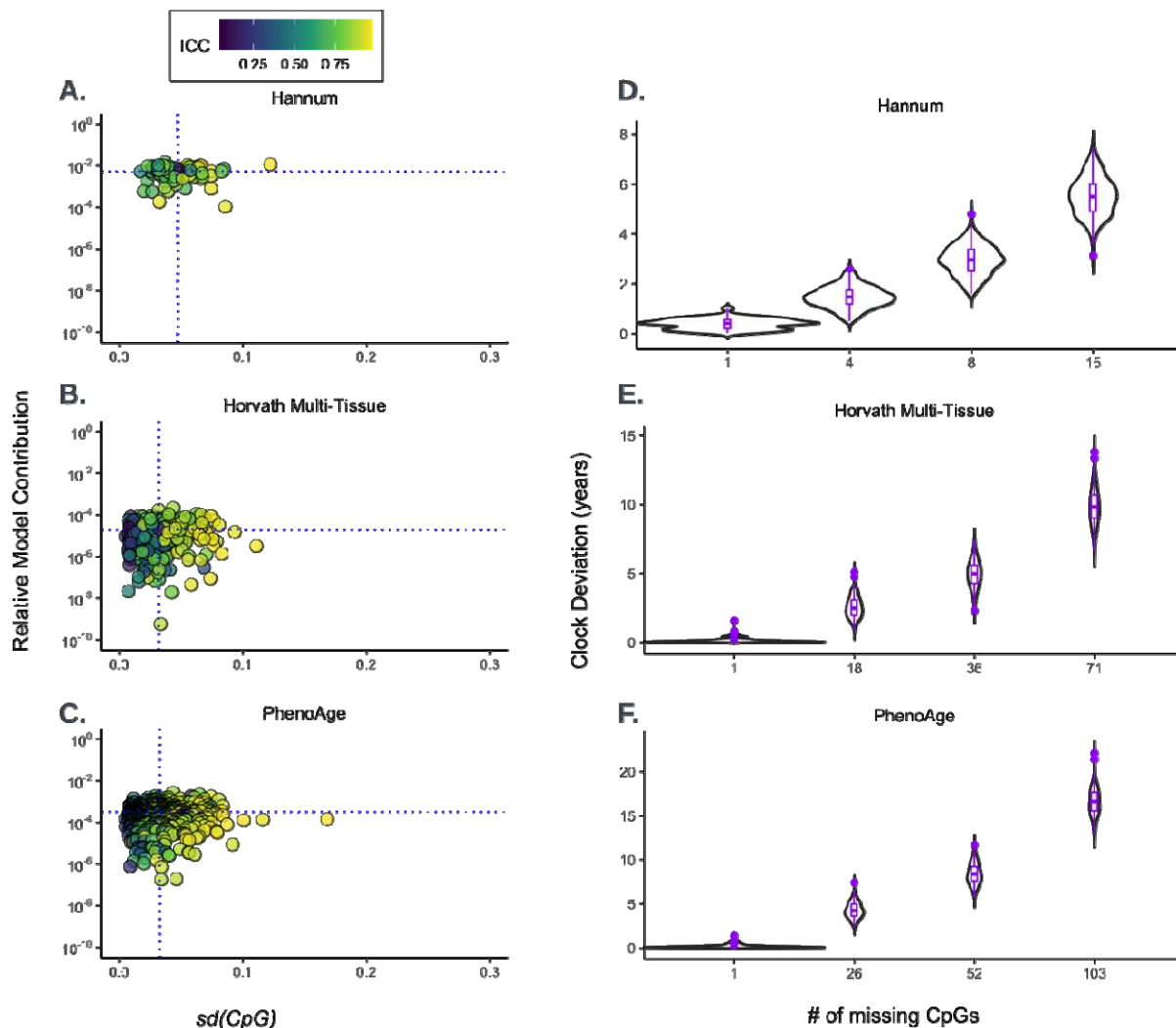
575

576 **Figure 1: The Evolution and Diversity of Epigenetic Clocks.** (A) Epigenetic clocks are semantically
577 organized into key categories, and (B) individual clocks categorized and highlighted along a timeline.
578 Note that years with multiple clocks are colored in blocks from top to bottom according to the alphabetical
579 list.



580

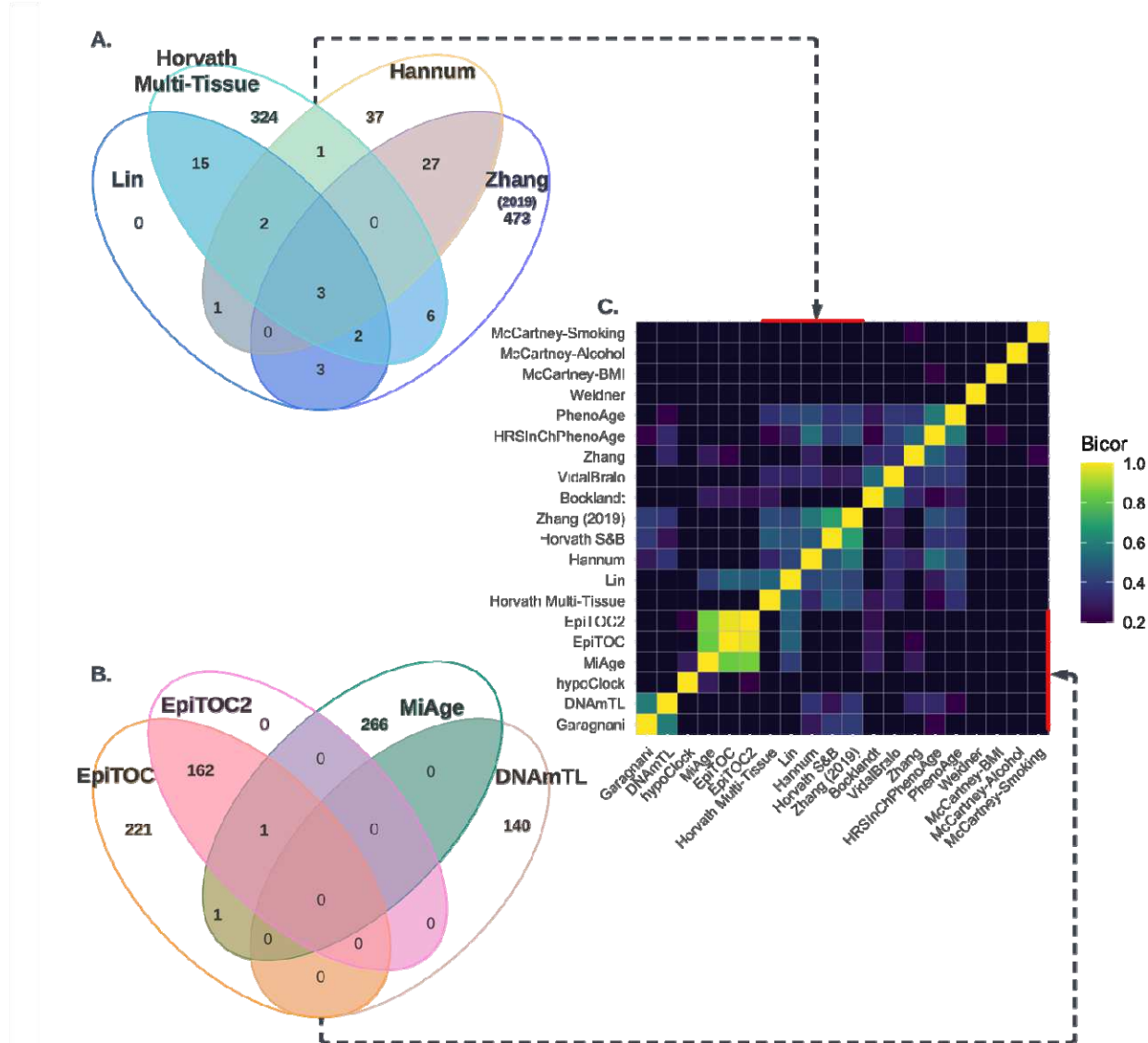
581 **Figure 2: methylCIPHER Function Schema.** A representational schematic of the functionality contained
 582 within methylCIPHER. Data is connected as inputs with dashed lines. User inputs are colored in yellow,
 583 with objects required to be supplied by the user highlighted with “!”. Orange rectangles indicate functions
 584 exported by methylCIPHER for the user to run. Blue pentagonal boxes indicate outputs, with green
 585 checkmarks as endpoints. Green cylindrical objects are RData objects stored and accessible from within
 586 the package.



587

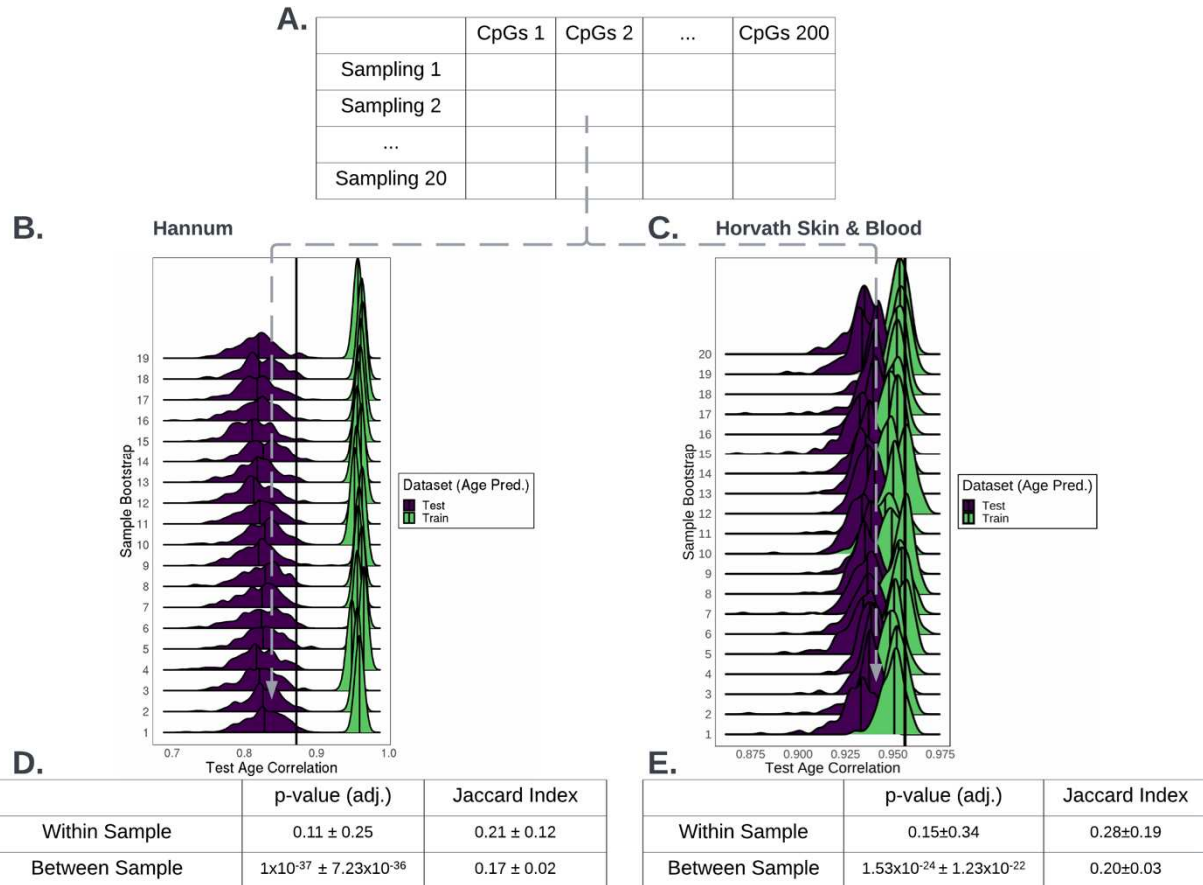
588 **Figure 3: Impacts of Missing CpG Imputation on Key Clocks.** Three representative clocks, Hannum
589 (A, D), Horvath Multi-Tissue (B, E), and PhenoAge (C, F), were selected to assess the effects of
590 imputation. Relative model contribution was calculated according to the absolute CpG weight in the
591 regression model, multiplied by the standard deviation of the CpG in the Framingham Heart Study
592 dataset. The model contributions of each CpG were plotted against the standard deviation of the CpGs,
593 with the mean of each axis plotted as a blue crosshatch (A-C). Imputation of CpGs in the top right
594 quadrant, with high standard deviation and high model contribution, will have a greater impact than CpGs
595 in the other quadrants. Further, clocks whose CpGs extend further into this region will be more impacted
596 by mean imputation effects. We repeatedly tested and plotted the effects of mean imputation on 0.1%,

597 5%, 10% and 20% of CpGs selected at random (**D-F**). Due to varying sizes of the clocks, these
598 percentages represent varying numbers of missing CpGs for each of the clocks.



599
600 **Figure 4: Shared Signal Does Not Arise From Shared CpGs.** Epigenetic clocks were selected from the
601 categories of highly accurate chronological age clocks (A) and cancer & mitotic rate clocks (B) as defined
602 in Figure 1. Selection of CpG identity overlap was limited to 4 clocks per category, and in the case of
603 mitotic clocks hypoClock was not included as it was designed to select different CpGs from EpiTOC2. (C)
604 Sex-adjusted clock residuals were found in FHS and correlated according to biweight midcorrelation

605 (thresholded at >0.2). While clock residuals can capture well-correlated information, their CpG overlaps
606 within a cluster can be quite low.

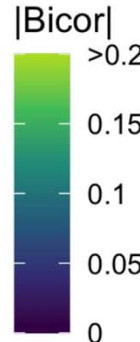
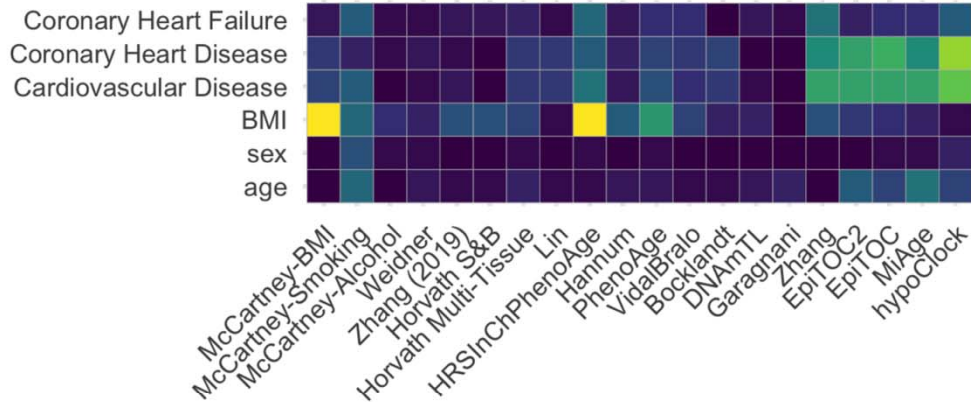


607

608 **Figure 5: Bootstrapping Methylation Data Demonstrates Methylation Redundancy.** The
 609 experimental design matrix (**A**) demonstrates how both samples (19x) and CpGs (200 x 10k CpGs) were
 610 selected with random amounts of overlap in their sampled dimensions. Each sampling cell was used to
 611 retrain an elastic net regression model of the Hannum (**B**) or the Horvath Skin & Blood (**C**) clocks. The
 612 large vertical lines demonstrate the correlation of the originally developed clock in the whole test dataset.
 613 Smaller vertical lines in the purple density plots indicate the median age correlation of the within-sample
 614 bootstrap elastic net trials. As each experiment is allowed to overlap in CpGs to an extent, we use the p-
 615 value and Jaccard indices of modified gene set overlap tests to determine whether CpGs are repeatedly
 616 selected across bootstrapped CpG lists and within a given list across sampling sets, for both Hannum (**D**)
 617 and Horvath Skin & Blood (**E**).

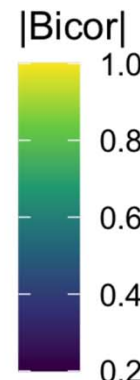
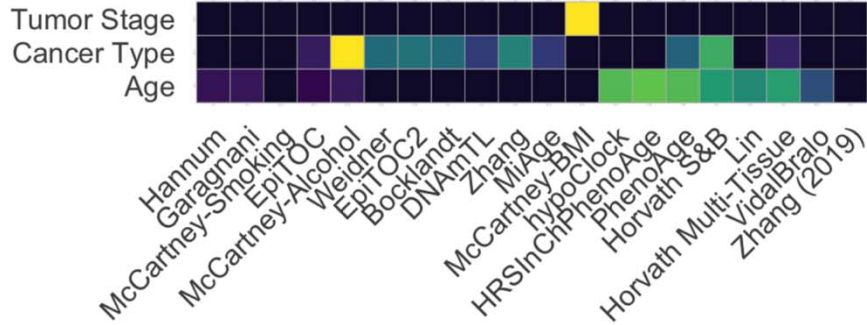
A.

Framingham Heart Study (FHS)



B.

The Cancer Genome Atlas (BRCA, KIRC, LUSC)



618

619 **Figure 6: Clock Univariate Associations Capture Key Signal In Diverse Datasets.** The available
620 epigenetic clocks' simple age regression (regression of clock onto just age) were converted to z-scores
621 across each dataset, as were samples metadata such as age, BMI, or sex. Additional sample traits were
622 left as original variables as z-scores aren't realistic. The univariate associations were then described as
623 the absolute biweight midcorrelation between the z-scored clock residuals and sample metadata. (A) In
624 FHS data, there is clear associations between traits of interest and a cluster of mitotic clocks, whereas (B)
625 in a few cancers in TCGA data, McCartney lifestyle/ trait predictors of Alcohol and BMI show the strongest
626 correlations to traits of interest.